Available online at www.sciencedirect.com
SCIENCE DIRECT®
PERGAMON
Polyhedron 22 (2003) 1091–1098
POLYHEDRON
www.elsevier.com/locate/poly

Nature of Fe^{III}–O_2, Fe^{II}–CO and Fe^{III}–CN complexes of hemoprotein models

Francisco Torrens *

Institut Universitari de Ciència Molecular, Universitat de València, Dr. Moliner 50, E-46100 Burjassot, Valencia, Spain

Received 18 November 2002; accepted 17 January 2003

Abstract

Parametrization of a molecular-mechanics program to include terms specific for 5- and 6-coordinate transition metal complexes results in computer-simulated structures of hemo complexes. The principal new feature peculiar to 5- and 6-coordination is a term that measures the effect of electron-pair repulsion modified by the ligand electronegativity and takes into account the different structural possibilities. The work consists in the modification of program molecular mechanics for 5- and 6-coordination. The model system takes into account the structural differences of the fixing centre in the haemoglobin (Hb) subunits. The customary proximal histidine is added. The macrocycle hemo IX is wholly considered in our model. The calculations show clearly that certain conformations are much more favourable that others for fixing O_2. From the O_2 binding in haemoglobin and myoglobin and in simple Fe porphyrin models it is concluded that the bent O_2 ligand is best viewed as bound superoxide, O_2^-.

Keywords: Electron-pair repulsion; Polarizing molecular mechanics; Iron–porphyrin complex; Heme charge; Oxygen fixation; CO/O_2 discrimination

1. Introduction

The heme group is in the active centre of a number of relevant proteins as the oxygen (O_2) transport proteins haemoglobin (Hb) and myoglobin (Mb) [1,2], as well as enzymes involved in catabolism as peroxidases [3], catalases, oxidases [4] and cytochromes [5]. The replacement of Fe by Mg in heme leads to chlorophyll [6], and the replacement of Fe by other transition metals coupled with modifications in the aromatic ring leads to species as vitamin B_{12} [7] and cofactor F-430 [8]. The study of heme models is a focal point of experimental bioinorganic chemistry [9].

Rohmer and co-workers characterized the electronic state of Fe(P) (P = porphyrin) complexes [10–12], and predicted an electronic structure, which was later proved by experiment [13]. Other theoretical studies are the real position of the CO group in Fe(P)(Im)(CO) (Im = imidazole) complexes [14,15], the position of the CN group in $Fe(mdi)_2(py)(CN)$ (mdi = malondialdiminate) complexes [16], the role of distal and proximal histidines (His) on the binding of O_2 in Hb [17–20], and structural aspects of the binding of O_2 and other ligands to heme [21–27]. The amount of information obtained from the calculations is seriously limited by the size of the heme group itself, which has allowed only recently the appearance of theoretical studies on reactivity [28–33].

The coordination of O_2 to the Fe(P)(Im) 5-coordinate species leads to 6-coordinate species with octahedral geometry, i.e., the biomimetic forms of Mb–O_2 and Hb–O_2. X-ray data were reported only on two complexes, $Fe(T_{piv}PP)[1\text{-(Me)Im}](O_2)$ [34] and $Fe(T_{piv}PP)[2\text{-(Me)Im}](O_2)$ [35]. Both complexes are quite similar, sharing the same porphyrin $T_{piv}PP$, which is *meso*-tetrakis(α,α,α,α-*o*-pivalamidophenyl)porphyrin. Maseras and co-workers optimized the geometry of $Fe(T_{piv}PP)[1\text{-(Me)Im}](O_2)$ with the hybrid quantum mechanics/molecular mechanics (QM/MM) method IMOMM(DFT-B3LYP:MM3) [36] and pure QM DFT-B3LYP [37]. Ghosh and Bocian optimized the geometry of Fe(P)(Im)(CO) with density functional theory (DFT) [19]. Salzmann et al. optimized under constraint the geometry of a $Fe(T_{piv}PP)[1\text{-(Me)Im}](CO)$ model with DFT-B3LYP [38]. Han et al. calculated a

* Tel.: +34-96-354-3182; fax: +34-96-354-3156.
E-mail address: francisco.torrens@uv.es (F. Torrens).

0277-5387/03/$ - see front matter © 2003 Elsevier Science Ltd. All rights reserved.
doi:10.1016/S0277-5387(03)00095-0

heme model–CO system employing the ab initio pseudopotential method with local density approximation (LDA) exchange correlation [39].

The reversibe binding of O_2 and carbon monoxide (CO) played a central role in studies of heme-protein structure and function. As a result, numerous encumbered Fe^{II} porphyrin models were synthesized in an effort to elucidate the structural details of small ligand binding. The steric bulk of certain axial ligands bonded to synthetic Fe^{II} porphyrins provided model compounds of reduced O_2 and CO affinity, and models of the so-called tense (T) state of hemoproteins. Unfortunatelly, thus far there is only one single-crystal X-ray structure determination on such a complex [40]. There was much discussion on the mechanistic basis of the variation of affinity values in heme proteins and model compounds. This focused on the nature of the axial ligand, distal steric effects, distal polar effects, and enforced doming and ruffling of the porphyrin skeleton. Johansson et al. showed by quantum chemical calculations on *a* haem a model that upon reduction the spin pairing at Fe is accompanied by effective delocalization of electrons from the Fe towards the periphery of the porphyrin ring, including its substituents [41,42].

In previous papers, both non-interacting (NID) and interacting (ID) induced-dipoles polarization models were implemented in the program molecular mechanics (MM2) [43]. The polarizing force field for proteins (MMID2) was described elsewhere [44] and applied to *N*-formylglycinamide (For-Gly-NH_2) [45,46]. In this work, MMID2 has been improved to include terms specific for 5- and 6-coordination. The new program is called MMIDX. Section 2 presents the computational method. Section 3 describes the improvements in the force field. Section 4 discusses the calculation results. Section 5 summarizes the conclusions.

2. Computational method

Molecular polarizabilities are calculated with the method of Applequist et al. [47]. The molecule consists of N atoms (i, j,...), each of which responds to an electric field by the induction of a dipole moment, which is a linear function of the local field. If a Cartesian component of the field is E_a^i, the induced moment in atom i is:

$$\mu_a^i = \alpha^i \left(E_a^i + \sum_{j(\neq i)}^{N} T_{ab}^{ij} \mu_b^j \right) \tag{1}$$

where α^i is the polarizability of atom i and T_{ab}^{ij} is the field gradient tensor, $T_{ab}^{ij} = (1/e)\nabla_a^i E_b^j$, e is the charge of the proton. Eq. (1) can be expressed:

$$\bar{\mu} = \bar{\bar{\alpha}}(\bar{\bar{I}}\bar{E} + \bar{\bar{T}}\bar{\mu}) = \bar{\bar{\alpha}}\bar{\bar{I}}\bar{E} + \bar{\bar{\alpha}}\bar{\bar{T}}\bar{\mu}$$

where $\bar{\bar{I}}$ is the $3N \times 3N$ dimensional unit matrix. The equation can be solved as

$$\bar{\mu} = (\bar{\bar{I}} - \bar{\bar{\alpha}}\bar{\bar{T}})^{-1}\bar{\bar{\alpha}}\bar{E} = \bar{\bar{A}}\bar{E}$$

Here, the symmetrical many-body polarizability matrix $\bar{\bar{A}}$ is introduced:

$$\bar{\bar{A}} = (\bar{\bar{I}} - \bar{\bar{\alpha}}\bar{\bar{T}})^{-1}\bar{\bar{\alpha}}$$

The compact matrix equation $\bar{\mu} = \bar{\bar{A}}\bar{E}$ is equivalent to the N matrix equations:

$$\bar{\mu}^i = \sum_{j=1}^{N} \bar{\bar{A}}^{ij}\bar{E}^j$$

If the molecule is in a uniform applied field ($\bar{E}^j = \bar{E}$), this equation becomes

$$\bar{\mu}^i = \left[\sum_{j=1}^{N} \bar{\bar{A}}^{ij} \right] \bar{E} = \bar{\bar{\alpha}}^{eff,i}\bar{E}$$

The coefficient of $\bar{E}$ is the effective polarizability of i, $\bar{\bar{\alpha}}^{eff,i}$. The total induced μ is:

$$\bar{\mu}^{mol} = \sum_{i=1}^{N} \bar{\mu}^i = \left[\sum_{i=1}^{N} \sum_{j=1}^{N} \bar{\bar{A}}^{ij} \right] \bar{E} = \left[\sum_{i=1}^{N} \bar{\bar{\alpha}}^{eff,i} \right] \bar{E}$$

from which it is seen that the molecular polarizability tensor $\bar{\bar{\alpha}}^{mol}$ is:

$$\bar{\bar{\alpha}}^{mol} = \sum_{i=1}^{N} \sum_{j=1}^{N} \bar{\bar{A}}^{ij} = \sum_{i=1}^{N} \bar{\bar{\alpha}}^{eff,\ i} \tag{2}$$

3. Force-field modifications

1,3-Interactions between atoms bonded to a common atom are not specifically included in Eq. (3) in the MM2+polarization approach because they are effectively already included in the bond-length and bond-angle *strainless* parameters.

$$E_{\text{steric}} = \sum E_{\text{str}} + \sum E_{\text{bend}} + \sum E_{\text{tors}} + \sum E_{\text{nb}} \tag{3}$$

However, for 5-coordinate structures, there is a need to consider the effect of 1,3-interactions because an energy term is needed for ligand–ligand repulsion (1) to account for the stability difference of various geometries possible, and (2) to account for structural effects due to the variation of ligand electronegativity. Since the geometries of the methylfluorophosphoranes $(CH_3)_nPF_{5-n}$ $(n = 0 \rightarrow 3)$ were qualitatively correlated with Gillespie's VSEPR theory, VSEPR was adopted as a model for the present approach. Bond electron-pair repulsion (EPR) terms were introduced via the non-bonded term E_{nb} of Eq. (3) modified to express EPR effects for atoms bonded to 5- or 6-coordinated atoms.

The unmodified non-bonded energy term is

$$E_{\mathrm{nb(AB)}} = \varepsilon\left[8.28\times10^{5}\,\exp\left(-\frac{1}{0.0736P}\right) - 2.25P^{6}\right] \quad (4)$$

where $P=[r_{\mathrm{VDW(A)}}+r_{\mathrm{VDW(B)}}]/r_{\mathrm{AB}}$, r_{VDW} is the van der Waals radius of the specific atom, and r_{AB} is the non-bonded distance between A and B; $\varepsilon=(\varepsilon_{\mathrm{A}}\varepsilon_{\mathrm{B}})^{1/2}$ where ε_{A} and ε_{B} are parameters specific to atoms A and B, and are related to the hardness of the atoms. Hill evaluated the constants in Eq. (4), which give the energy $E_{\mathrm{nb(AB)}}$ in units of kilocalories per mole [48].

The modification of Eq. (4) to express 1,3-bond EPR terms is [49]

$$E_{(1,3)\mathrm{AB}} = D\varepsilon\left[8.28\times10^{5}\,\exp\left(-\frac{1}{0.0736P^{*}}\right) - 2.25P^{*6}\right] \quad (5)$$

The addition of a scaling factor D, to obtain a suitable balance between the energy of this 1,3-term and the other energy terms in Eq. (3), and the replacement of P with P^{*} (where $P^{*}=[r_{\mathrm{VDW(A)}}+r_{\mathrm{VDW(B)}}]/r^{*}_{\mathrm{AB}}$ and r^{*}_{AB} is the distance between atoms A and B calculated from modified bond lengths, d^{*}_{CA} and d^{*}_{CB}, between the central atom C and either atom A or B) provide the necessary adjustments to quantitatively reproduce the $(CH_3)_nPF_{5-n}$ structures [50]. The variation in ligand electronegativity is introduced by a distance factor R_A in the relation $d^{*}_{\mathrm{CA}}=d_{\mathrm{CA}}R_{\mathrm{A}}$. The magnitude of R is inversely related to the electronegativity difference between atoms C and A. The R factors are the means of including the concept of bond EPR between atoms A and B. If the electronegativity difference ΔX_{CA} is large, the bonding electron pair can be considered to move away from atom C, thus decreasing the bond EPR between the C–A and C–B bonds. When $\Delta X_{\mathrm{CA}} > \Delta X_{\mathrm{CA'}}$, the repulsion term $E_{(1,3)\mathrm{AB}} < E_{(1,3)\mathrm{A'B}}$ even when the actual bond lengths are equal. A set of distance factors R may be obtained from the bond ionic character I,

$$I = 1-\exp\left[-\frac{1}{4}(\Delta X_{\mathrm{CA}})^{2}\right] \quad (6)$$

and using the relation

$$R=\frac{Ir_{\mathrm{A}}+r_{\mathrm{C}}}{r_{\mathrm{A}}+r_{\mathrm{C}}} \quad (7)$$

where r_{A} and r_{C} are covalent radii of atoms A and C.

4. Calculation results and discussion

The structure of heme(–His)–O_2 is shown in Fig. 1. Heme is the prostetic group of Hb. The van der Waals parameters for the Fe atom have been taken from the UFF force field [51], and the torsional contributions involving dihedral angles with the metal atom and the bending terms involving Fe in central position have been set to zero. The dipole moment increases, in general, with the oxidation state of Fe. Therefore, the dipole moment of Fe^{III} heme(–His)–O_2 and –CN results large due to the polar $Fe^{\delta+}$–O–$O^{\delta-}$ and $Fe^{\delta+}$–C–$N^{\delta-}$ complexes, respectively. The binding of His in heme and of CN in heme–His increase the dipole moment.

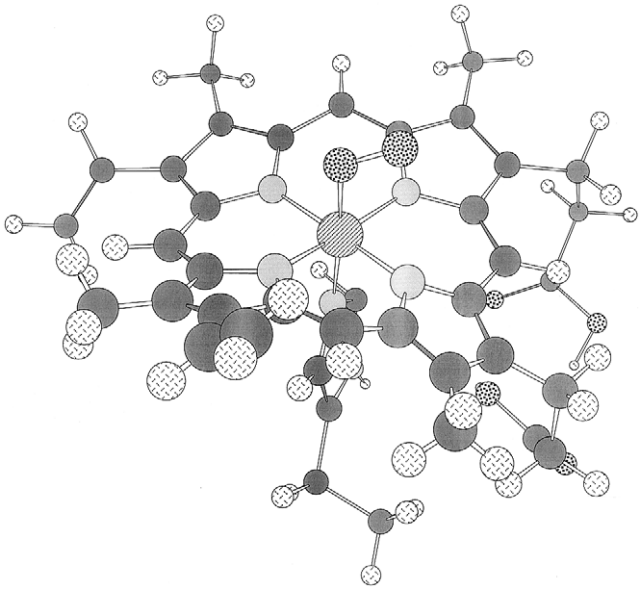

Fig. 1. Structure of heme(–His)–O_2. Heme is the prostetic group of haemoglobin.

4.1. The 4-coordinate Fe(P) system

The heme group has little direct application in biochemistry, but it is a natural starting point for both experimental and theoretical studies. The crystal structures of a number of heme derivatives were reported, with different substituents in the ring. The simplest model, with all substituents being H atoms, was not provided. Because of this, comparison will be made with a species containing some substituents. In particular, Fe(TPP) (TPP = *meso*-tetraphenylporphyrin) has been chosen. Its electronic state is well known experimentally to correspond to a low spin triplet ($S=1$). Selected structural parameters are collected in Table 1. The agreement in bond angles between both MM2/MMX+polarization geometries and the X-ray structure is good, with discrepancies always smaller than 5°. Discrepancies in bond distances are larger in a number of cases. This is the case of the C–C_{bridge}, C–C′ and C′–C″ distances. These distances have values of 1.395, 1.439 and 1.365 Å, respectively, in X-ray, approximately 1.336, 1.340 and 1.332 Å, respectively, in MM2/MMX+polarization. Agreement between experiment

Table 1
Selected geometric parameters (Å and °) from the geometry optimization of Fe(P) with the pure B3LYP and with the IMOMM(B3LYP:MM3) methods [37]

	MM2	MM2+NID [a]	MM2+ID [b]	MMX [c]	MMX [c]+NID [a]	MMX [c]+ID [b]
Fe–N [d]	1.881	1.878	1.877	1.881	1.878	1.877
N–C	1.353	1.352	1.350	1.353	1.352	1.350
C–C_{bridge}	1.337	1.336	1.334	1.337	1.336	1.334
C–C′	1.341	1.340	1.339	1.341	1.340	1.339
C′–C″	1.332	1.332	1.332	1.332	1.332	1.332
Fe–N–C	128.6	128.6	128.6	128.6	128.6	128.6
N–Fe–N	90.2	90.2	90.2	90.2	90.2	90.2
N–C–C_{bridge}	120.8	120.8	120.9	120.8	120.8	120.9
N–C–C′	112.0	112.1	112.1	112.0	112.1	112.1
	Experiment	Pure QM	QM/MM			
Fe–N	1.966	2.016	1.940			
N–C	1.378 [d]	1.397	1.362			
C–C_{bridge}	1.395 [d]	1.402	1.369			
C–C′	1.439 [d]	1.459	1.345			
C′–C″	1.365 [d]	1.367	1.333			
Fe–N–C	127.2 [d]	127.4	127.7			
N–Fe–N	90.0 [d]	90.0	90.0			
N–C–C_{bridge}	125.3 [d]	125.5	126.2			
N–C–C′	110.6 [d]	110.4	110.3			

Experimental data on the Fe(TPP) system are also provided for comparison [13].
[a] NID, polarization by non-interacting induced dipoles.
[b] ID, polarization by interacting induced dipoles.
[c] Scaling factor $D = 0.2$.
[d] Average values.

and MM2/MMX+polarization is good (≈ 0.06 Å). All these atoms are in part purely described with MM2, and the optimized MM2/MMX+polarization values are close to the optimal bond distance for these types of atoms in the applied force field, which is 1.337 Å. Another discrepancy in the geometries appears in the Fe–N distance. This is more puzzling, because the calculated distance 1.877–1.881 Å is smaller than the experimental value of 1.966 Å.

4.2. The 5-coordinate Fe(P)(Im) system

Coordination of an Im ligand to the heme group leads to a 5-coordinate species with a square pyramidal geometry. These compounds are good biomimetic models of Mb and Hb, the Im replacing the proximal His of the biological systems. The need to avoid both the dimerization and the formation of the 6-coordinate species with two axial ligands poses serious restrictions on the nature of the porphyrins able to give this kind of complexes. For this study, the species Fe(Piv_2C_8)[1-(Me)Im] {Piv_2C_8 = α,α,5,15-[2,2′-(octanediamido)diphenyl]-α,α,10,20-bis(*o*-pivalamidophenyl)porphyrin} has been chosen. This species has the advantage of having 1-methylimidazole as axial ligand, in contrast with the more common 2-methylimidazole, which is more sterically demanding. Unfortunately, neither for Fe(Piv_2C_8)-[1-(Me)Im] nor for other 5-coordinate derivatives of heme the electronic state is experimentally known. Electronic spectroscopy, magnetic susceptibility and Mössbauer measurements are conclusive in identifying it as high spin ($S = 2$). Selected parameters are resumed in Table 2. The Fe–$N_{porphyrin}$ distances are longer by approximately 0.06 Å (MMX) than those in the 4-coordinate system. This trend is in agreement with the reference values. This result is fully consistent with the shift from low spin to high spin in the metal. Most data focus on the description of the Im. Overall agreement in the geometric parameters is correct. Moreover, one has to take with some suspicion the X-ray parameters of the Im, which would make the N=C double bond N_{Im}–C_{Im} of Im longer than the N–C single bond N_{Im}–C'_{Im}. However, the MMX+polarization calculations are, in general, in agreement with the QM/MM reference, which provides the expected result.

The sharper discrepancy concerns the $N_{porphyrin}$–Fe–N_{Im}–C_{Im} dihedral angle. This angle measures the rotation around the Fe–N_{Im} single bond, and rules the placement of the Im plane with respect to the porphyrin ring. Its sign is arbitrary, because the x and y directions are equivalent in absence of axial ligand. In this work, a positive sign has been chosen for consistence with data on the 6-coordinate complexes presented below. An angle of 90° (like in the pure QM reference) means that

Table 2
Selected geometric parameters (Å and °) from the geometry optimization of Fe(P)(NH=CH_2) with the pure B3LYP and of Fe(P)[1-(Me)Im] with the IMOMM(B3LYP:MM3) methods [37]

Parameter	MM2	MM2+NID [a]	MM2+ID [b]	MMX [c]	MMX [c]+NID [a]	MMX [c]+ID [b]
Fe–$N_{porphyrin}$ [d]	1.897	1.894	1.890	1.945	1.926	1.923
Fe–N_{Im}	1.866	1.863	1.864	1.964	1.905	1.919
N_{Im}–C_{Im}	1.327	1.327	1.326	1.491	1.446	1.473
N_{Im}–C'_{Im}	1.344	1.343	1.338	1.505	1.492	1.469
Fe–N_{Im}–C_{Im}	126.3	126.3	126.1	119.4	119.3	108.2
Fe–N_{Im}–C'_{Im}	126.7	126.6	126.3	132.8	117.4	155.9
$N_{porphyrin}$–Fe–N_{Im}–C_{Im}	115.8	115.7	114.9	133.8	92.4	92.6
Parameter	Experiment	Pure QM	QM/MM			
Fe–$N_{porphyrin}$	2.074	2.101	2.029			
Fe–N_{Im}	2.134	2.252	2.233			
N_{Im}–C_{Im}	1.350	1.279	1.299			
N_{Im}–C'_{Im}	1.250	– [e]	1.414 [f]			
Fe–N_{Im}–C_{Im}	127.0	126.1	136.8			
Fe–N_{Im}–C'_{Im}	120.0	120.6	122.6			
$N_{porphyrin}$–Fe–N_{Im}–C_{Im}	126.0	90.0	133.2			

Experimental data on the Fe(Piv_2C_8)[1-(Me)Im] system are also provided for comparison [53].
[a] NID, polarization by non-interacting induced dipoles.
[b] ID, polarization by interacting induced dipoles.
[c] Scaling factor $D = 0.2$.
[d] Average values.
[e] Frozen in calculation.
[f] Corresponds to N–H in this calculation.

the Im plane is eclipsing one of the Fe–$N_{porphyrin}$ bonds, while an angle of 135° (approximately the 133.8° found with MMX) indicates a staggered orientation of the Im with respect to the Fe–$N_{porphyrin}$ bonds. Therefore, both pure QM and MMX values are just opposite with the experimental value (126.0°) lying in between, although closer to the MMX value. The MMX+polarization results lie, in general, in the range 90°–133° of the references. The importance of the large discrepancy between different values is, however, arguable, because there is also a large dispersion in different experimental 5-coordinate derivatives of heme, as well as in experimental reports of Mb and Hb. It seems, therefore, that the rotation around this single bond has a very low barrier.

4.3. The 6-coordinate Fe(P)(Im)(O_2), Fe(P)(Im)(CO) and Fe(P)(Im)(CN) systems

Coordination of O_2 to the 5-coordinate heme–His species leads to 6-coordinate species with an octahedral geometry. These compounds are the biomimetic forms of Mb–O_2 and Hb–O_2. X-ray data are reported only on two complexes, Fe(T_{piv}PP)[1-(Me)Im](O_2) and Fe(T_{piv}PP)[2-(Me)Im](O_2). Both complexes are quite similar, sharing the same porphyrin T_{piv}PP, which is *meso*-tetrakis(α,α,α,α-*o*-pivalamidophenyl)porphyrin. The Fe(T_{piv}PP)[1-(Me)Im](O_2) complex, containing the less sterically demanding 1-methylimidazole ligand, has been chosen for comparison. The state of this system is a low spin open-shell singlet ($S = 1$) resulting in a Fe^{III}–O_2^- charge distribution. Selected parameters are reported in Table 3. The parameters concerning the coordination of O_2, which are probably the most critical for the biochemical activity of Hb, are well reproduced. The computed values for the Fe–O distance, 1.8–1.9 Å, are close to the experimental value of 1.746 Å. The calculated values (1.21–1.35 Å) for the O–O distance are far from the experimental report of 1.163 Å. However, the experimental value (even shorter than the 1.21 Å for free O_2) is suspect, because of the disorder on the placement of the second O atom within the crystal, as admitted by the authors of the X-ray experiment themselves [34]. The O–O interatomic distance increases from 1.21 Å in free O_2 to 1.326 Å (MMX+ID), suggesting that electronic charge is transferred from FeP to O_2, in agreement with the experimental result that the Fe–O_2 bond can be formally described as Fe^{III}–O_2^- [9].

A similar reasoning can be used for the Fe–O–O bond angles, which are, nevertheless, in all cases indicative of a bent η^1 coordination mode, where only one O atom is directly attached to the metal.

The sharper discrepancy concerns the $N_{porphyrin}$–Fe–O–O dihedral angle. This angle measures the rotation around the Fe–O single bond, and rules the placement of the Fe–O–O plane with respect to the porphyrin ring. An angle of 0° (approximately the 3.3° with MM2)

Table 3
Selected geometric parameters (Å and °) from the geometry optimization of Fe(P)(NH=CH_2)(O_2) with the pure B3LYP and of Fe(P)[1-(Me)Im](O_2) with the IMOMM(B3LYP:MM3) methods [37], and of Fe(T_{piv}PP)(Im)(O_2) with LSD [21]

Parameter	MM2	MM2+NID [a]	MM2+ID [b]	MMX [c]	MMX [c]+NID [a]	MMX [c]+ID [b]
Fe–$N_{porphyrin}$ [d]	1.880	1.876	1.870	1.964	1.948	1.933
Fe–N_{Im}	1.871	1.862	1.861	1.932	2.027	1.901
Fe–O	1.847	1.841	1.845	1.931	1.968	1.925
O–O	1.211	1.210	1.210	1.354	1.353	1.326
Fe–O–O	123.5	121.5	122.8	127.5	134.5	131.3
O–Fe–N_{Im}	171.7	169.5	168.6	131.0	120.4	157.2
$N_{porphyrin}$–Fe–N_{Im}–C_{Im}	179.0	178.2	176.8	155.7	159.0	149.5
$N_{porphyrin}$–Fe–O–O	3.3	5.0	16.5	32.9	35.0	5.4
Parameter	Experiment	Pure QM	QM/MM	LSD		
Fe–$N_{porphyrin}$	1.978	2.035	1.949	2.010		
Fe–N_{Im}	2.070	2.050	2.167	2.070[e]		
Fe–O	1.746	1.757	1.759	1.770		
O–O	1.163	1.268	1.286	1.300		
Fe–O–O	129.4	121.1	117.0	121.0		
O–Fe–N_{Im}	180.0	175.8	179.4	–		
$N_{porphyrin}$–Fe–N_{Im}–C_{Im}	159.5	177.9	137.0	–		
$N_{porphyrin}$–Fe–O–O	42.4	44.6	44.1	–		

Experimental data on the Fe(T_{piv}PP)[1-(Me)Im](O_2) system are also provided for comparison [34].
[a] NID, polarization by non-interacting induced dipoles.
[b] ID, polarization by interacting induced dipoles.
[c] Scaling factor $D = 0.2$.
[d] Average values.
[e] Frozen in calculation.

Table 4
Selected distances (Å) from the complete geometry optimization of Fe(P)(Im)(CO) with LDA [39], partial geometry optimization of Fe(T_{piv}PP)[1-(Me)Im](CO) with DFT (B3LYP and BPW91) [38], and complete geometry optimization of Fe(mdi)$_2$(py)(CO) with NLDFT [16], of Fe(P)(Im)(CO) with LDFT [37] and of Fe(T_{piv}PP)(Im)(CO) with LSD [21]

Parameter	MM2	MM2+NID [a]	MM2+ID [b]	MMX [c]	MMX [c]+NID [a]	MMX [c]+ID [b]	
Fe–$N_{porphyrin}$ [d]	1.878	1.873	1.871	1.945	1.959	1.935	
Fe–N_{Im}	1.868	1.863	1.862	1.963	2.071	2.067	
Fe–C	1.971	1.970	1.970	2.033	2.193	2.160	
C–O	1.110	1.109	1.110	1.198	1.211	1.205	
Fe–C–O	180.0	180.0	180.0	179.5	174.5	166.9	
C–Fe–N_{Im}	179.7	174.6	174.3	171.0	146.1	143.7	
$N_{porphyrin}$–Fe–N_{Im}–C_{Im}	136.0	178.9	176.0	166.2	140.8	159.1	
Parameter	Experiment	LDA	B3LYP	BPW91	NLDFT	LDFT	LSD
Fe–$N_{porphyrin}$	2.003	1.990	–	–	1.961	1.983	2.020
Fe–N_{Im}	2.071	1.960	–	–	2.139	1.966	2.070[e]
Fe–C	1.793	1.790	1.801	1.743	1.739	1.733	1.720
C–O	1.095	1.160	1.147	1.167	1.166	1.165	1.170
Fe–C–O	179.3	180.0	180.0	180.0	180.0	180.0	180.0
C–Fe–N_{Im}	178.3	180.0	180.0	180.0	180.0	180.0	–
$N_{porphyrin}$–Fe–N_{Im}–C_{Im}	–	174.2	–	–	–	–	–

Experimental data on the Fe(T_{piv}PP)[1-(Me)Im](CO) system are also provided for comparison [38].
[a] NID, polarization by non-interacting induced dipoles.
[b] ID, polarization by interacting induced dipoles.
[c] Scaling factor $D = 0.2$.
[d] Average values.
[e] Frozen in calculation.

means that the Fe–O–O plane is eclipsing one of the Fe–$N_{porphyrin}$ bonds, while an angle of 45° (approximately the 44.6° in the pure QM reference) indicates a staggered orientation of the O_2 with respect to the Fe–$N_{porphyrin}$ bonds. The MMX/MMX+NID results lie near the reference results.

Selected structural parameters of Fe(P)(Im)(CO) are shown in Table 4. The geometric parameters concerning the coordination of CO, which are probably the most critical for the biochemical activity of Hb, are well reproduced. The computed values for the Fe–C distance, 2.0–2.2 Å, are close to the experimental value of 1.793 Å. The calculated values (1.1–1.2 Å) for the C–O distance are close to the experimental report of 1.095 Å. The C–O interatomic distance is similar in the free molecule (1.171 Å, calculated with AM1 [52]) and 1.198 Å (MMX), suggesting that electronic charge is not transferred from FeP to CO. This is in agreement with the experimental result that the Fe–CO bond can be formally described as Fe^{II}–CO [9]. The global energy minimum occurs at a linear geometry for Fe–C–O (MM2+polarization and MMX). These calculations are in agreement with the experiment and calculation references.

The rotation of the Im side chain is significant. The Im ring is rotated so that the N atom is directed toward the Fe atom, and the rotation angle $N_{porphyrin}$–Fe–N_{Im}–C_{Im} reaches approximately 176° (MM2+polarization) in agreement with the LDA reference (174.2°).

However, for heme(–His)–CN, the C–N distance increases from 1.147 Å (AM1) in free CN to 1.16–1.28 Å, suggesting that electronic charge is transferred from FeP to CN. This is in agreement with the experimental result that the Fe–CN bond can be formally described as Fe^{III}–CN^- [9]. A linear Fe^{III}–CN^- binding model is proposed.

5. Conclusions

From the preceding results the following conclusions can be drawn.

1) For the heme-IX adducts, the NID or ID polarization energy represents 74% of the total energy MM2+polarization. The EPR energy corresponds to 48% of the total energy MMX+polarization.
2) The model system takes into account the structural differences of the fixing centre in the Hb subunits. The calculations show that certain conformations are much more favourable that others for fixing O_2.
3) Three different Fe-binding models are proposed for O_2, CO and CN: bent superoxide Fe^{III}–O_2^-, linear Fe^{II}–CO and linear Fe^{III}–CN^-. The nature of O_2 binding in Hb, Mb and simple Fe–porphyrin models is becoming clear. When O_2 is bound as a bent, rather than a triangular, ligand, it is best described as bound superoxide. This bent geometry may be critical to biological functioning because it allows the discrimination between O_2 and CO.

Acknowledgements

The author acknowledges financial support of the Spanish MCT (Plan Nacional I+D+I, Project No. BQU2001-2935-C02-01).

References

[1] M.F. Perutz, Proc. R. Soc. London, B 208 (1980) 135.
[2] M.F. Perutz, G. Fermi, B. Liusi, B. Shaanan, R.C. Liddington, Acc. Chem. Res. 20 (1987) 309.
[3] K.G. Welinder, Curr. Opin. Struct. Biol. 2 (1992) 388.
[4] B.G. Malmström, Chem. Rev. 90 (1990) 1247.
[5] M. Sono, M.P. Roach, E.D. Coulter, J.H. Dawson, Chem. Rev. 96 (1996) 2841.
[6] J. Barber, B. Andersson, Nature (London) 370 (1994) 31.
[7] C.L. Drennan, S. Huang, J.T. Drummond, R.G. Matthews, M.L. Ludwig, Science 266 (1994) 1669.
[8] M.A. Halcrow, G. Christou, Chem. Rev. 94 (1994) 2421.
[9] M. Momenteau, C.A. Reed, Chem. Rev. 94 (1994) 659.
[10] A. Dedieu, M.-M. Rohmer, A. Veillard, Adv. Quantum Chem. 16 (1982) 43.
[11] M.-M. Rohmer, A. Dedieu, A. Veillard, Chem. Phys. 77 (1983) 449.
[12] M.-M. Rohmer, Chem. Phys. Lett. 116 (1985) 44.
[13] N.Y. Li, Z. Su, P. Coppens, J. Landrum, J. Am. Chem. Soc. 112 (1990) 7294.
[14] T.G. Spiro, P.M. Kozlowski, J. Biol. Inorg. Chem. 2 (1997) 516.
[15] T.G. Spiro, P.M. Kozlowski, J. Am. Chem. Soc. 120 (1998) 4524.
[16] T. Vangberg, D.F. Bocian, A. Ghosh, J. Biol. Inorg. Chem. 2 (1997) 526.
[17] P. Jewsbury, S. Yamamoto, T. Minato, M. Saito, T. Kitagawa, J. Am. Chem. Soc. 116 (1994) 11586.
[18] P. Jewsbury, S. Yamamoto, T. Minato, M. Saito, T. Kitagawa, J. Phys. Chem. 99 (1995) 12677.
[19] A. Ghosh, D.F. Bocian, J. Phys. Chem. 100 (1996) 6363.
[20] E. Sigfridsson, U. Ryde, J. Biol. Inorg. Chem. 4 (1999) 99.
[21] C. Rovira, P. Ballone, M. Parrinello, Chem. Phys. Lett. 271 (1997) 247.
[22] C. Rovira, K. Kunc, J. Hutter, P. Ballone, M. Parrinello, J. Phys. Chem. A 101 (1997) 8914.
[23] C. Rovira, K. Kunc, J. Hutter, P. Ballone, M. Parrinello, Int. J. Quantum Chem. 69 (1998) 31.
[24] C. Rovira, M. Parrinello, Chem. Eur. J. 5 (1999) 250.
[25] C. Rovira, P. Carloni, M. Parrinello, J. Phys. Chem. B 103 (1999) 7031.
[26] R. Salzmann, M.T. McMahon, N. Godbout, L.K. Sanders, M. Wojdelski, E. Oldfield, J. Am. Chem. Soc. 121 (1999) 3818.
[27] N. Godbout, L.K. Sanders, R. Salzmann, R.H. Havlin, M. Wojdelski, E. Oldfield, J. Am. Chem. Soc. 121 (1999) 3829.
[28] G. Loew, M. Dupius, J. Am. Chem. Soc. 118 (1996) 10584.
[29] D.L. Harris, G.H. Loew, J. Am. Chem. Soc. 118 (1996) 10588.
[30] D. Harris, G. Loew, L. Waskell, J. Am. Chem. Soc. 120 (1998) 4308.
[31] D.E. Woon, G.H. Loew, J. Phys. Chem. A 102 (1998) 10380.
[32] O. Zakharieva, M. Grodzicki, A.X. Trautwein, C. Veeger, I.M.C.M. Rietgens, J. Biol. Inorg. Chem. 1 (1996) 192.

[33] M.T. Green, J. Am. Chem. Soc. 120 (1998) 10772.
[34] G.B. Jameson, G.A. Rodley, W.T. Robinson, R.R. Gagne, C.A. Reed, J.P. Collman, Inorg. Chem. 17 (1978) 850.
[35] G.B. Jameson, F.S. Molinaro, J.A. Ibers, J.P. Collman, J.I. Brauman, E. Rose, K.S. Suslick, J. Am. Chem. Soc. 102 (1980) 3224.
[36] F. Maseras, New J. Chem. 22 (1998) 327.
[37] J.-D. Maréchal, G. Barea, F. Maseras, A. Lledós, L. Mouawad, D. Pérahia, J. Comput. Chem. 21 (2000) 282.
[38] R. Salzmann, C.J. Ziegler, N. Godbout, M.T. McMahon, K.S. Suslick, E. Oldfield, J. Am. Chem. Soc. 120 (1998) 11323.
[39] S. Han, K. Cho, J. Ihm, Phys. Rev. E 59 (1999) 2218.
[40] K. Kim, J. Fettinger, J.L. Sessler, M. Cyr, J. Hugdahl, J.P. Collman, J.A. Ibers, J. Am. Chem. Soc. 111 (1989) 403.
[41] M.P. Johansson, M.R.A. Blomberg, D. Sundholm, M. Wikström, Biochim. Biophys. Acta 1553 (2002) 183.
[42] M.P. Johansson, D. Sundholm, G. Gerfen, M. Wikström, J. Am. Chem. Soc. 124 (2002) 11771.
[43] N.L. Allinger, J. Am. Chem. Soc. 99 (1977) 8127.
[44] F. Torrens, M. Ruiz-López, C. Cativiela, J.I. García, J.A. Mayoral, Tetrahedron 48 (1992) 5209.
[45] F. Torrens, J. Sánchez-Marín, J.-L. Rivail, An. Fís. (Madrid) 90 (1994) 197.
[46] F. Torrens, Mol. Simul. 24 (2000) 391.
[47] J. Applequist, J.R. Carl, K.-K. Fung, J. Am. Chem. Soc. 94 (1972) 2952.
[48] T.L. Hill, J. Chem. Phys. 16 (1948) 399.
[49] J.A. Deiters, J.C. Gallucci, T.E. Clark, R.R. Holmes, J. Am. Chem. Soc. 99 (1977) 5461.
[50] H. Yow, L.S. Bartell, J. Mol. Struct. 15 (1973) 209.
[51] A.K. Rappé, C.J. Casewit, K.S. Colwell, W.A. Goddard, III, W.M. Skiff, J. Am. Chem. Soc. 114 (1992) 10024.
[52] M.J.S. Dewar, E.G. Zoebisch, E.F. Healy, J.J.P. Stewart, J. Am. Chem. Soc. 107 (1985) 3902.
[53] M. Momenteau, W.R. Scheidt, C.W. Eigenbrot, C.A. Reed, J. Am. Chem. Soc. 110 (1988) 1207.